Acta Biomaterialia 46 (2016) 29–40

Contents lists available at ScienceDirect

Acta Biomaterialia

journal homepage: www.elsevier.com/locate/actabiomat

Full length article

Self-assembling peptide hydrogel for intervertebral disc tissue engineering

Simon Wan [a,*], Samantha Borland [a,b], Stephen M. Richardson [c], Catherine L.R. Merry [a,d], Alberto Saiani [a], Julie E. Gough [a]

[a] School of Materials, University of Manchester, Manchester M13 9PL, UK
[b] Division of Cardiovascular Sciences, School of Medical Sciences, Faculty of Biology, Medicine and Health, University of Manchester, Manchester M13 9PL, UK
[c] Division of Cell Matrix Biology and Regenerative Medicine, School of Biological Sciences, Faculty of Biology, Medicine and Health, University of Manchester, Manchester M13 9PL, UK
[d] Wolfson Centre for Stem Cells, Tissue Engineering and Modelling, Centre for Biomolecular Sciences, University of Nottingham, University Park, Nottingham NG7 2RD, UK

ARTICLE INFO

Article history:
Received 14 May 2016
Received in revised form 12 September 2016
Accepted 23 September 2016
Available online 24 September 2016

Keywords:
Self-assembling peptide hydrogel
Degenerative disc disease
Low back pain
Nucleus pulposus
Cell-based therapy
Regenerative medicine

ABSTRACT

Cell-based therapies for regeneration of intervertebral discs are regarded to hold promise for degenerative disc disease treatment, a condition that is strongly linked to lower back pain. A *de novo* self-assembling peptide hydrogel (SAPH), chosen for its biocompatibility, tailorable properties and nanofibrous architecture, was investigated as a cell carrier and scaffold for nucleus pulposus (NP) tissue engineering. Oscillatory rheology determined that the system would likely be deliverable via minimally invasive procedure and mechanical properties could be optimised to match the stiffness of the native human NP. After three-dimensional culture of NP cells (NPCs) in the SAPH, upregulation of NP-specific genes (*KRT8*, *KRT18*, *FOXF1*) confirmed that the system could restore the NP phenotype following de-differentiation during monolayer culture. Cell viability was high throughout culture whilst, similarly to NPCs *in vivo*, the viable cell population remained stable. Finally, the SAPH stimulated time-dependent increases in aggrecan and type II collagen deposition, two important NP extracellular matrix components. Results supported the hypothesis that the SAPH could be used as a cell delivery system and scaffold for the treatment of degenerative disc disease.

Statement of Significance

Lower back pain (LBP) prevalence is widespread due to an aging population and the limited efficacy of current treatments. As LBP is strongly associated with intervertebral disc (IVD) degeneration, it is thought that cell-based therapies could alleviate LBP by repairing IVD tissue.

Various natural and synthetic biomaterials have been investigated as potential IVD tissue engineering scaffolds. Self-assembling peptide hydrogels (SAPHs) combine advantages of both natural and synthetic biomaterials; for example they are biocompatible and have easily modifiable properties.

The present study demonstrated that a *de novo* SAPH had comparable strength to the native tissue, was injectable, restored the IVD cell phenotype and stimulated deposition of appropriate matrix components. Results illustrated the promise of SAPHs as scaffolds for IVD tissue engineering.

1. Introduction

Lower back pain (LBP) affects as much as 84% of people in their lifetime [1] with the cost to the UK economy estimated at £12 billion per annum [2]. LBP aetiology is multi-factorial, with genetics [3], mechanical injury [4] and aging all contributing to the condition. However intervertebral disc (IVD) degeneration, also known as degenerative disc disease (DDD), is strongly associated with LBP in over 40% of cases [5].

The IVD consists of 3 distinct but interdependent tissues; the fibrous annulus fibrosus (AF) which surrounds the gelatinous nucleus pulposus (NP) [6] with cartilage end-plates on the superior and inferior surfaces [7]. The main roles of the IVD are to act as a shock absorbing system by transferring loads and dissipating

* Corresponding author.
E-mail addresses: simon.wan@manchester.ac.uk (S. Wan), samantha.borland@postgrad.manchester.ac.uk (S. Borland), s.richardson@manchester.ac.uk (S.M. Richardson), cathy.merry@nottingham.ac.uk (C.L.R. Merry), a.saiani@manchester.ac.uk (A. Saiani), j.gough@manchester.ac.uk (J.E. Gough).

http://dx.doi.org/10.1016/j.actbio.2016.09.033
1742-7061/

energy that the spine is subjected to [8], and to act as joints [9]. DDD occurs when there is an imbalance between IVD extracellular matrix (ECM) catabolic and anabolic events [10] which often leads to an inflammatory reaction [11].

Current LBP treatments have limited long-term efficacy [12] and crucially are symptomatic rather than curative. LBP prevalence is rising due to an aging population [13] so there is an urgent need for an entirely new approach DDD treatment.

DDD originates within the NP [14] therefore it has been hypothesised that restoration of a degenerated NP when a healthy AF is present may slow DDD, provide analgesic effects and restore mobility of the back [7] whilst still preserving the capacity of the IVD to remodel [15,16]. A number of animal model trials that investigated the transplantation of NP cells (NPCs) into artificially degenerated IVDs have produced promising results [17] with increases in ECM production and maintenance of disc height reported [18–20]. Injection of autologous human IVD derived chondrocytes into the NPs of LBP sufferers determined that, after a 2 year follow-up, cell therapy provided superior analgesic effects and higher fluid levels than the control population [21].

Due to the disadvantages of current biomaterials, such as lack of biocompatibility and issues with matching the biomechanics of native tissue [22,23], self-assembling peptide hydrogels (SAPHs) have been investigated as potential NP tissue engineering cell carriers and scaffolds. SAPHs have the inherent ability to self-assemble into complex supramolecular structures after exposure to the appropriate stimuli [24,25]. The simple self-assembly mechanism produces hydrogels suitable for the culture of a number of cell lines [22,26,27]. In theory, SAPHs combine the advantages of natural and synthetic biomaterials whilst overcoming their deficiencies [23,28]. For example, the peptide sequence can be easily modified to control the final mechanical and structural properties [22] whilst SAPHs are likely to display good biocompatibility as their breakdown products will be the same as those of proteins synthesised *in vivo*.

A number of SAPH classes have been investigated for applications in NP tissue engineering with promising biocompatibility results reported however these studies did not investigate the rheological behaviour of the SAPHs despite the important biomechanical role of the NP [29–31]. Furthermore, these (and similar) NP SAPH studies used a limited and non-NP specific set of marker genes [29–32] therefore the phenotype of the encapsulated cells could not be confirmed. We have previously identified a number of novel genes that characterize the bovine IVD transcriptional profiles, allowing determination of a NPC phenotype [33].

FEFEFKFK (F; phenylalanine, E; glutamic acid, L; lysine) chains have a hydrophobic and hydrophilic face [24,27] so an increase in solution ionic strength and pH causes the chains to self-assemble into anti-parallel β-sheets nanofibres. Above a critical gelation concentration, the nanofibres aggregate into a self-supporting hydrogel accompanied by a significant increase in viscosity and slight reduction in volume [22]. FEFEFKFK SAPHs have been successfully exploited as drug delivery vehicles [34] and cell culture scaffolds [27,35]. Bovine articular chondrocytes encapsulated within FEFEFKFK SAPH adopted rounded morphology, proliferated and produced the cartilage ECM component type II collagen which suggested that cells retained their phenotype. It was concluded that the system was a suitable bovine chondrocyte culture environment and could serve as a template for cartilage tissue engineering [36]. Previous studies have highlighted a strong similarity in cell morphology and ECM production between chondrocytes and NPCs [33,37]. We postulated that the FEFEFKFK SAPH should therefore be capable of supporting NPC culture, preserving their phenotype and stimulating production of appropriate ECM components.

In this study, FEFEFKFK SAPH was investigated for its potential as a cell carrier and scaffold for NP tissue engineering. The system was characterised then optimised to match the native NP strength and to determine its injectability. Finally, the 3D culture of primary bovine NPCs was analysed for cell viability, gene expression of encapsulated cells and production of ECM components to determine whether the FEFEFKFK SAPH could restore and preserve the NP phenotype.

2. Materials & methods

2.1. Preparation of SAPH

Table 1 describes the FEFEFKFK SAPH production process where the predetermined amount of peptide powder (>95% purity, batch LR294429) (*Biomatik, USA*) was dissolved in distilled water (dH_2O). The samples (pH 1.9–2.1) were heated at 80 °C for 2 h to ensure complete dissolution. The gelation process was induced by the addition of 1 M NaOH and 100 μl of 10× Dulbecco's phosphate buffered solution (DPBS) (*HyClone, USA*). Further heating at 80 °C for 12 h aided mixing of constituents. Cooling to room temperature (RT) produced a homogenous clear hydrogel with a pH of between 9.3 and 9.6.

2.2. Oscillatory rheology to determine viscoelastic properties

Viscoelastic behaviour was determined using an AR-G2 rheometer with 20 mm parallel plates on days 1, 7 and 14 after plating FEFEFKFK SAPH (Section 2.4). For each run, 150 μl of sample was loaded onto the stage and the upper plate was lowered to a 0.25 mm gap. A strain amplitude sweep was performed at constant frequency (1 Hz) between 0.01 and 100% strain to determine the linear viscoelastic region of the material. The storage modulus (G′), the deformation energy stored during the shear process of the sample [38], and loss modulus (G″), the amount of energy dissipated during shear [24], was recorded at 1% strain (frequency sweep). A recovery cycle experiment on day 1, designed to mimic the injection process, involved breaking the SAPH by applying 160% strain then reducing the strain to 1% and recording G′ and G″ values. All samples were tested at 37 °C and a solvent trap was used to minimise solvent evaporation.

2.3. Bovine NPC isolation and culture

Bovine NPCs (bNPCs) were isolated from bovine tails (18–36 months) purchased from a local abattoir. Each sample was enzymatically digested in serum-free media containing 0.5% pronase (*Merck Chemicals Ltd, Nottingham, UK*) for one hour and transferred to serum free media containing 0.5% collagenase type II (*Invitrogen, Paisley, UK*) and 0.1% hyaluronidase (*Sigma, Poole, UK*) for two to three hours on an orbital shaker at 37 °C. Supernatant

Table 1
Constituents required to produce 25, 30 and 35 mg ml^{-1} FEFEFKFK SAPHs.

Final SAPH concentration/mg ml^{-1}	Peptide powder/mg	dH_2O/μl	1M NaOH/μl	10× DPBS/μl	Cell suspension or medium/μl
25	31.25	811	89	100	250
30	37.5	802	98	100	250
35	43.75	786	114	100	250

was passed through a 40 μm filter to remove any tissue debris. BNPCs were expanded under standard culture conditions in high glucose Dulbecco's Modified Eagle's medium (*PAA, Austria*) supplemented with 10% (v/v) foetal bovine serum (FBS), 1% (v/v) penicillin and 1% (v/v) streptomycin (*Sigma-Aldrich, USA*). At 80%–90% confluence, cells were sub-cultured using 0.05% trypsin–0.53 mM ethylenediaminetetraacetic acid (EDTA)4Na solution (*Gibco–Invitrogen, UK*) and transferred to a Falcon tube to recover the cell pellet by centrifugation. The cell pellet was re-suspended in fresh medium, cells were counted and volume adjusted to the required cell concentration.

2.4. 3D seeding of FEFEFKFK SAPHs

FEFEFKFK SAPHs were sterilised for 30 min using ultra violet (UV) radiation. 250 μl of cell suspension containing either 2.5×10^5 bNPC ml^{-1} or 1.875×10^6 bNPCs ml^{-1} at passage 4–6 was mixed with the FEFEFKFK SAPH ensuring a homogenous distribution of cells so the final cell density was either 2×10^5 - bNPCs ml^{-1} or 1.5×10^6 bNPCs ml^{-1} of FEFEFKFK SAPH. For acellular samples used in rheology experiments, 250 μl of medium was added to FEFEFKFK SAPHs instead of cell suspension. The predetermined peptide powder amounts in Table 1 have been adjusted so that addition of 250 μl cell suspension produced the final desired FEFEFKFK SAPH concentration. 450 μl of sample was pipetted into a 12-well Millicell® cell culture insert (*Millipore, UK*) then fresh media was added. Samples were then incubated at 37 °C (20% O_2, 5% CO_2). Every 25 min for a total of 125 min, the cell culture media was changed to return the FEFEFKFK SAPHs to a physiologically relevant pH. Media was subsequently exchanged every 2 days and samples were cultured under standard conditions.

2.5. Cell viability

Cell viability was assessed using LIVE/DEAD® assay (*Invitrogen, UK*) on days 1, 3, 7 and 14 after cell encapsulation. Samples were incubated in PBS supplemented with 10 mM calcein AM and 1 mM ethidium homodimer-1 for 15 min at 37 °C. The solution was removed and samples were imaged using a Leica TCS SP5 confocal microscope (*Leica Microsystems, Germany*) and LASAF software. 200 μm stacks were imaged at 5 μm intervals along the axial plane and 500 μm stacks were imaged at 5 μm intervals along the sagittal plane.

2.6. Total viable cell numbers (CytoTox 96® cytotoxicity assay)

Viable cell numbers were determined using CytoTox 96® cytotoxicity assay (*Promega, UK*) on days 1, 3, 7 and 14 after cell encapsulation. Cells in FEFEFKFK SAPH were lysed using a freeze-thaw process then 50 μl of supernatant was mixed with 50 μl of substrate assay mix. Samples were covered and incubated for 30 min at RT. Stop solution was added then absorbance was measured on an Ascent microplate reader at 492 nm wavelength. A standard curve was produced using known cell numbers then total viable cells was calculated.

2.7. DNA quantitation assay (Quant-iT™ Picogreen® dsDNA assay)

PicoGreen® reagent was prepared using a 1:200 dilution with TE buffer (10 mM Tris-HCl, 1 mM EDTA, pH 7.5) and protected from light. A DNA standard curve (0.1–1000 ng ml^{-1}) was prepared using known DNA concentrations.

A lysis buffer step was not required as the encapsulated cells had been papain digested (in preparation for Blyscan™ GAG assay Section 2.10). In triplicate, 100 μl of sample, blank and DNA standard dilutions were pipetted into a black 96-well plate. 100 μl of PicoGreen® working solution was then added into each well and mixed. Samples were incubated at RT for 4 min and protected from light. The plate was analysed on an FLx800 microplate reader (*BioTEK, USA*) with the fluorescence being measured using filters with a 485 nm excitation and a 538 nm emission wavelength. A standard curve was plotted using known cell number against fluorescence.

2.8. Determining gene expression

On days 1, 7 and 14 after cell encapsulation, the entire SAPH sample was transferred to a microcentrifuge tube and 1 ml of TRIzol® reagent (*Life Technologies, UK*) was added. The sample was mechanically disrupted and incubated for 15 min. RNA was isolated from bNPCs according to the manufacturer's instructions and quantified using a NanoDrop ND-1000 spectrophotometer (*NanoDrop Technologies, USA*). cDNA was prepared using the ABI high capacity kit (*Applied Biosystems, USA*) and diluted to 5 ng μl^{-1}.

Quantitative real time polymerase chain reaction (qRT-PCR) was performed to analyse gene expression using the Applied Biosystems StepOne Plus™ real-time PCR system. Reactions were prepared in triplicate to a total volume of 20 μl containing SYBR® Green mastermix (*Thermo Fisher Scientific, USA*), molecular grade H_2O, 600 nM of each primer [33] and 10 ng of cDNA. Primer sequences are provided in Table 2. Target gene expression was normalised to GAPDH and expressed as $2-\Delta CT$.

2.9. Visualisation of extracellular matrix components

Immunocytochemistry (ICC) was used to stain for aggrecan, and collagen I and II on days 3 and 7 after cell encapsulation. Samples were fixed with 4% (w/v) paraformaldehyde (PFA) for 30 min at RT. Then bNPCs were permeabilised using 0.05% (v/v) Triton X-100 in PBS for 15 min and blocked with 1% (w/v) bovine albumin serum (BSA) in PBS for 1 h. Samples were incubated overnight at 4 °C with the appropriate primary antibody; rabbit polyclonal to collagen type I (ab34710), rabbit polyclonal to collagen type II (ab34712) (*Abcam, UK*) or mouse monoclonal to aggrecan (7D4) (*AbD Serotec, USA*) at a dilution of 1:100, 1:200 and 1:500 respectively. Samples were then incubated for 90 min at RT in the dark using secondary goat anti-rabbit IgG-AlexaFluor 594 (1:500 dilution in BSA) (*Thermo Fisher Scientific, USA*) for type I and II collagen samples and secondary goat anti-mouse IgG AlexaFluor 568 (1:500 dilution) (*Thermo Fisher Scientific, USA*) for aggrecan samples. AlexaFluor 488 phalloidin (1:150 dilution) stained for F-actin. Between each step, samples were washed 5 times with DPBS. Samples were cured using DAPI-ProLong anti-fade and imaged using Leica TCS SP5 confocal microscope and LASAF software.

2.10. Quantification of total sulphated glycosaminoglycans

Total sulphated glycosaminoglycans (s-GAG) content was measured using Blyscan™ Glycosaminoglycan Assay (*Biocolor, UK*) which utilised 1, 9-dimethyl methylene blue (DMMB) to bind to s-GAGs. FEFEFKFK SAPHs were papain digested overnight at 65 °C on days 1, 3, 7 and 14 after cell encapsulation, then dye reagent was added to the samples and mechanically mixed for 30 min. After centrifuging, the bound pellet was dissociated and the s-GAG was recovered using a dissociation agent containing sodium dodecyl sulphate. Absorbance was measured using a Multiskan plate reader at 656 nM. Quant-iT PicoGreen® assay (*Invitrogen, USA*) (Section 2.7) was carried out on the same samples to determine cell number and s-GAG production per cell was calculated.

Table 2
Quantitative RT-PCR primer sequences.

Gene	Forward primers (5′-3′)	Reverse primers (5′-3′)
Glyceraldehyde 3-phosphate dehydrogenase (*GAPDH*)	TGCCGCCTGGAGAAA CC	CGCCTGCTTCACCACC TT
Aggrecan (*ACAN*)	GGGAGGAGACGACTG CAATC	CCCATTCCGTCTTGTTT TCTG
Type I collagen (*COL1A2*)	CTGTTCTGTTCCTTGTGTAACTGTGTT	GCCCCGGTGACACATCAA
Type II collagen (*COL2A1*)	CGGGCTGAGGGCAACA	CGTCAGCCATCCTTCAGA
Transcription factor SOX9 (*SOX9*)	GGGAAGCCTCACATCGACTTC	GGACATTACCTCATGGCTGATCT
Keratin 8 (*KRT8*)	ACCAGGAGCTCATGAATGTCAA	TCGCCCTCCAGCAGCTT
Keratin 18 (*KRT18*)	AAGGCCAGCTTGGAGAACAG	TTGAGCTGCTCCATCTGCAT
Forkhead Box F1 (*FOXF1*)	TCCCTCCCCACCTCAGAAGT	TGGCTTCAGAAATGCAAGTTACTC
Carbonic anhydrase 12 (*CA12*)	CCAACAACGGCCACTCAGT	CCCCGGACCTGCATGTC

2.11. Compositional analysis of chondroitin sulphate/dermatan sulphate (CS/DS)

1.5×10^6 bNPCs ml^{-1} were seeded into 30 mg ml^{-1} FEFEFKFK SAPHs as described in Section 2.4. After 5 days, media containing 50 μCi/ml of [^{3}H]-glucosamine (*PerkinElmer, USA*) was added to 3 separate FEFEFKFK SAPHs to generate metabolically radiolabelled GAGs as used previously [39]. On day 7 (48 h after [^{3}H]-glucosamine addition), the entire SAPH and cell culture media was transferred to a falcon tube, and the final volume adjusted to 20 ml with 1× PBS. Samples were digested with 200 μg/ml pronase for 4 h at 37 °C, and vortexed periodically to aid digestion of the SAPH. GAG chains were isolated by anion-exchange chromatography. In brief, samples were loaded onto a 1 ml diethylaminoethanol (DEAE) (*Sigma-Aldrich, USA*) column, washed with 0.25 M NaCl to remove weakly bound contaminants, and bound GAGs eluted with 1.5 M NaCl, monitoring for radiolabel using a Wallac 1409 liquid scintillation counter (*PerkinElmer, USA*). Eluted GAGs were pooled and de-salted using a PD-10 disposable Sephadex G-25M size exclusion column (*GE Healthcare, UK*) eluted in dH_2O, and lyophilised. For CS/DS disaccharide compositional analysis, recovered GAGs were digested with 2 mU chondroitinase ABC (*AMSBio, UK*) using 2 mU enzyme in 500 μl 50 mM Tris, 50 mM NaCl (pH 7.9) over 12 h and separated from non-digested GAG using size exclusion chromatography (Superdex 30, *Fischer Scientific, UK*); radioactivity was monitored as above. The eluted CS/DS disaccharides were then pooled and lyophilised. An aliquot (10,000 cpm of ^{3}H) of CS/DS disaccharides was applied to a Hypersil 5 μm column (*Thermo Scientific, USA*) and analysed by SAX-HPLC. Disaccharides were eluted with a 45 min linear gradient of 0–0.7 M NaCl in HPLC-grade water (pH 3.5) at a flow rate of 1 ml/minute. Fractions of 0.5 ml were collected and analysed by scintillation counting. Disaccharides were identified by comparison of elution position with known standards (*Iduron, UK*). The relative contribution of each disaccharide was expressed as a percentage of the total counts.

2.12. Preparation and seeding of alginate hydrogels

Alginate gels were used as positive controls for cell viability and cell population experiments on days 1 and 7 after encapsulation. The 2×10^5 bNPCs were re-suspended in 450 μl 30 mg ml^{-1} alginate solution (*Fisher Scientific, UK*). The homogenous suspension was added to a cell culture insert surrounded by 100 mM $CaCl_2$ solution (*Sigma-Aldrich, USA*) where gelation occurred. After 10 min, $CaCl_2$ was removed, gels were washed with 0.9% NaCl solution then fresh media was added to the samples which were cultured under standard conditions.

2.13. Statistical analysis

Statistical analysis was performed using one-way ANOVA to determine significant statistical differences between data. All data was expressed as mean ± standard deviation (SD) apart from gene expression results where data was expressed as mean ± standard error (SE). A significant P value is indicative of a significant difference where the probability is less than 0.05 ($^*P < 0.05$), 0.01 ($^{**}P < 0.01$) and 0.001 ($^{***}P < 0.001$).

3. Results

3.1. Characterising and optimising FEFEFKFK SAPH mechanical properties

Oscillatory rheology determined that for acellular FEFEFKFK SAPHs at 10 Hz, 25 mg ml^{-1} had G′ value of 6.4 ± 0.3 kPa, 30 mg ml^{-1} had G′ value of 19.6 ± 6.7 kPa and 35 mg ml^{-1} had G′ value of 51.1 ± 9.5 kPa on day 1 (Fig. 1A). For cell laden FEFEFKFK SAPHs at 10 Hz, 25 mg ml^{-1} had G′ value of 8 ± 0.4 kPa, 30 mg ml^{-1} had G′ value of 21.4 ± 2.9 kPa and 35 mg ml^{-1} had G′ value of 41.1 ± 8.6 kPa on day 1. There were no significant differences in G′ values on day 1 for cell-laden and cell-free FEFEFKFK SAPHs at 30 mg ml^{-1} and 35 mg ml^{-1} concentrations (Fig. 1A). All concentrations experienced significant decreases in G′ values with increasing time point for example at 1 Hz, G′ was 16.9 ± 1.8 kPa on day 1 compared to 4.3 ± 1.8 kPa on day 14 for 30 mg ml^{-1} concentration. However, G′ remained around 2–8 times higher than G″ for all samples due to FEFEFKFK SAPH always exhibiting predominantly elastic behaviour (G′ > G″) (Fig. 1B).

The dynamic modulus (|G*|) represents the total resistance of the material to deformation when repeatedly sheared and is analogous to stiffness. The |G*| value for acellular and cell-laden 30 mg ml^{-1} FEFEFKFK SAPH over a range of 1–100 rad s^{-1} was not significantly different to native non-degenerate NPs as measured by Iatridis et al. (Fig. 1C) [8]. 25 mg ml^{-1} FEFEFKFK SAPHs displayed comparable stiffness to the native NP of 5.39 kPa measured by Cloyd et al. [7]. The phase angle (δ) indicates energy dissipation during shearing. At 10 rad s^{-1}, the δ value of the native NP was 24° which indicated that it was visco-elastic with a dominant elastic component but still displayed a high viscous component [8]. At the same frequency on day 1, the δ value of 7.2 ± 0.9° for cell-laden FEFEFKFK SAPH meant that the system was less viscous and more elastic than the native NP.

3.2. Recovery cycles

The recovery cycle (Fig. 2A) was designed to simulate the injection process; the sample was sheared by applying a 160% strain to replicate the FEFEFKFK SAPH being forced through a needle (G′ < G″). A 1000 μl pipette tip (inner diameter of 0.78 mm) was typically used to plate samples whilst a 19G needle (inner diameter of 0.69 mm) was also used. When the strain was reduced to 1%, G′ > G″ within 6 s and the FEFEFKFK SAPH recovered its original

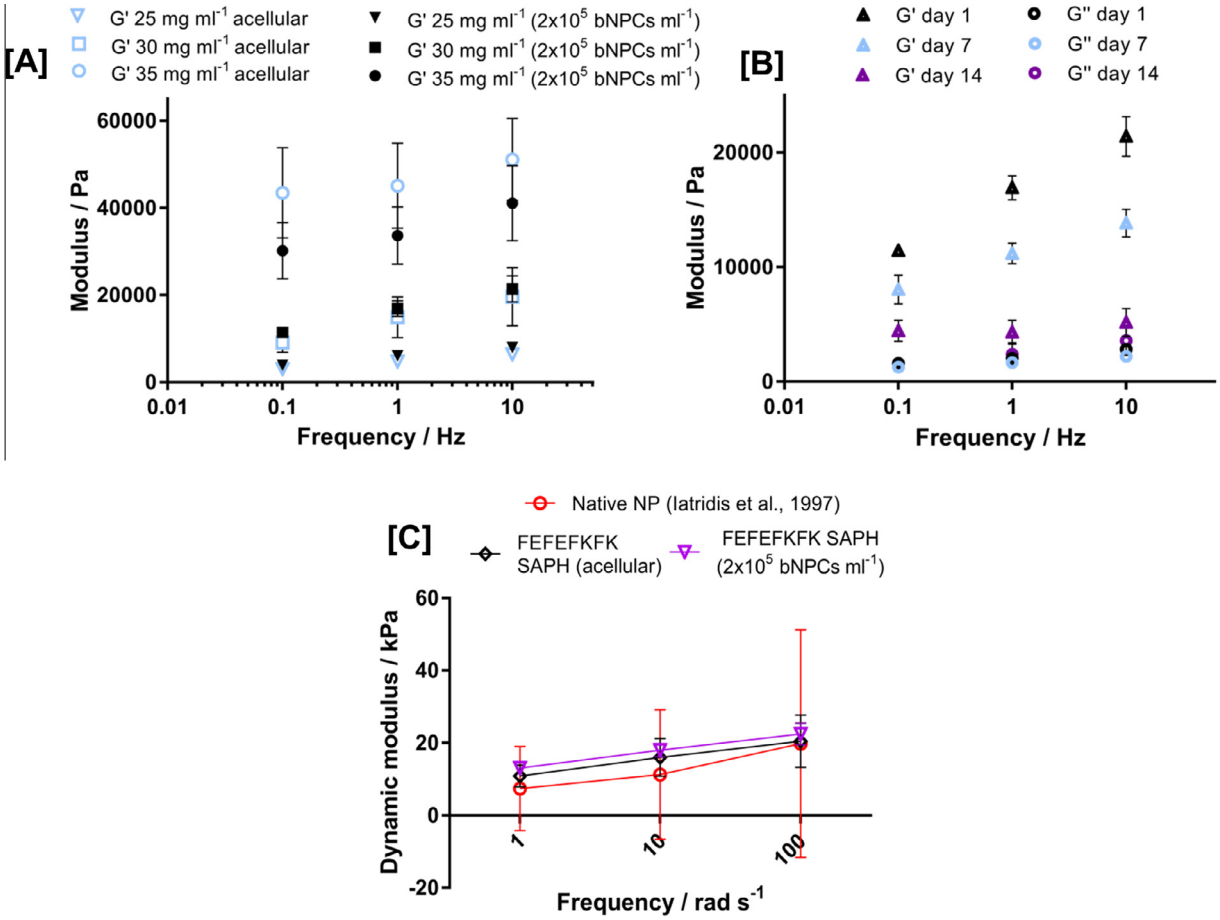

Fig. 1. Mechanical properties of acellular and cell-laden FEFEFKFK SAPH and comparison of system to native human NP. [A] Frequency sweep data for acellular and cell-laden 25, 30 and 35 mg ml^{-1} FEFEFKFK SAPH on day 1. [B] Frequency sweep data for 2 × 10^5 bNPCs ml^{-1} in 30 mg ml^{-1} FEFEFKFK SAPH on days 1, 7 and 14. [C] Dynamic modulus comparison of the native NP (red) as determined by Iatridis et al., acellular 30 mg ml^{-1} FEFEFKFK SAPH (black) and 30 mg ml^{-1} FEFEFKFK SAPH with 2 × 10^5 bNPCs ml^{-1} (purple). SAPHs at pH 7.4. FEFEFKFK SAPH values expressed as mean ± SD where n = 3. (For interpretation of the references to colour in this figure legend, the reader is referred to the web version of this article.)

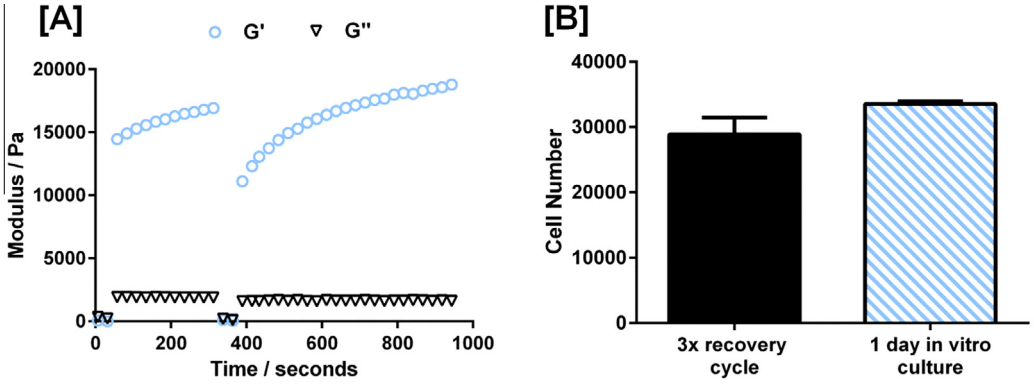

Fig. 2. Injectability of FEFEFKFK SAPH. [A] Recovery cycles for 2 × 10^5 bNPCs ml^{-1} in 30 mg ml^{-1} FEFEFKFK SAPHs at pH 7.4 after 1 day of *in vitro* culture. [B] Cell numbers calculated using CytoTox 96® non-radioactive cytotoxicity assay for 30 mg ml^{-1} FEFEFKFK SAPHs with 2 × 10^5 bNPCs ml^{-1}. There was no significant difference between cell population after 1 day of *in vitro* cell culture and after cells had been subjected to recovery cycles ($P > 0.05$). Values expressed as mean ± SD where n = 3.

stiffness within a few minutes. The ability of the FEFEFKFK SAPH to shear thin followed by self-heal was repeatable at least twice on the same sample. There was no significant difference in cell numbers on day 1 for samples subjected to 3 recovery cycles in comparison to control samples that did not undergo recovery cycles (Fig. 2B).

3.3. Assessing cell viability

There was a majority of viable bNPCs present for 25, 30 and 35 mg ml^{-1} FEFEFKFK SAPH concentrations at all time points (Fig. 3A). The proportion of viable cells present in fluorescence micrographs was 68.2 ± 4.1% for 25 mg ml^{-1}, 80 ± 6.4% for

30 mg ml^{-1} and was 73.7 ± 1.7% for 35 mg ml^{-1} on day 7 (Fig. 3B). Accordingly, 30 mg ml^{-1} concentration was chosen to continue with cell culture experiments where there was no significant difference in percentage viable cells comparing day 1–14 (Fig. 3C).

No significant changes in viable cell population were detected from days 1 (5.8×10^5 bNPCs) to 7 (4.6×10^5 bNPCs). There were no significant differences in cell number at any time point when comparing the culture of bNPCs in FEFEFKFK SAPHs and alginate controls (Fig. 3D).

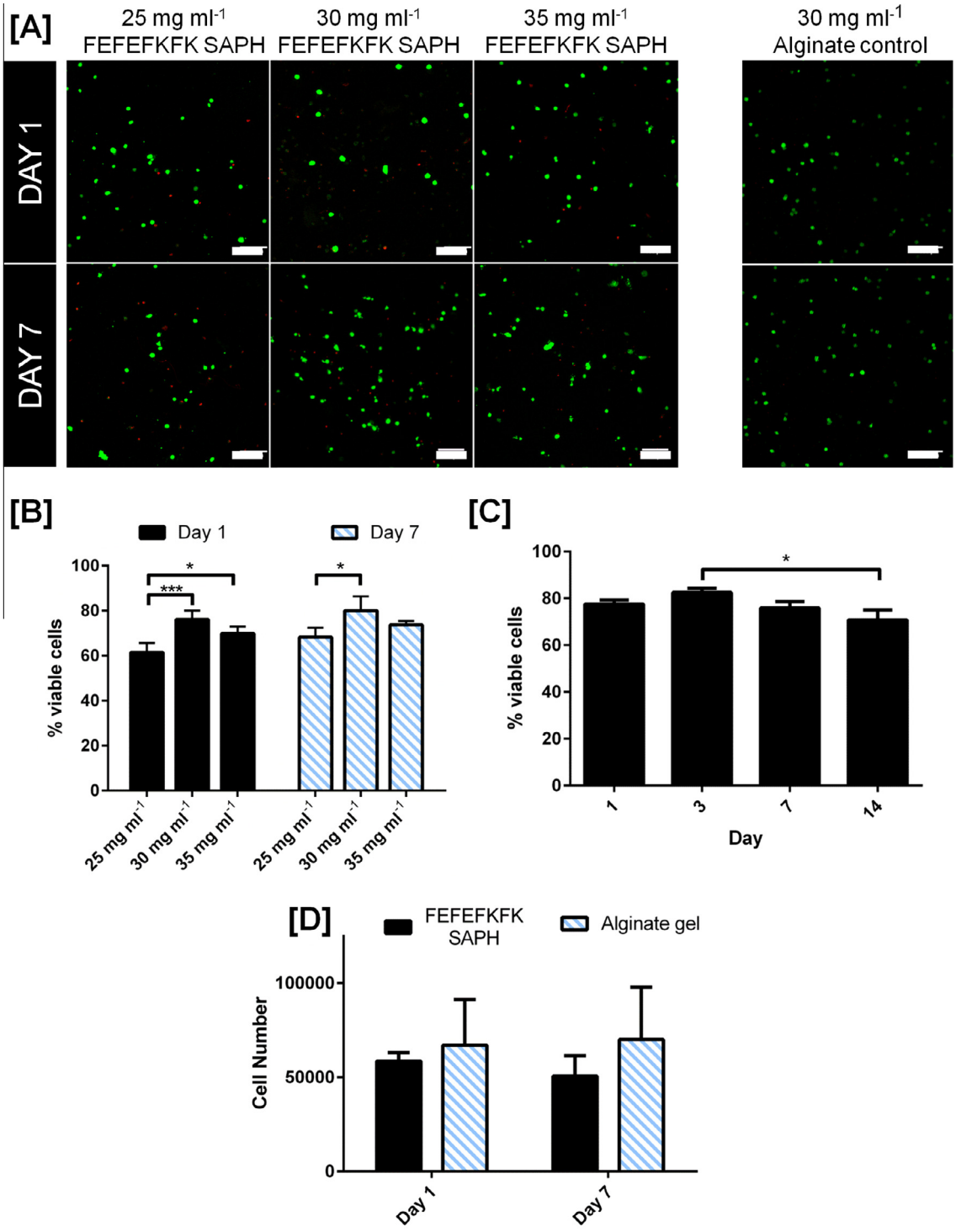

Fig. 3. Bovine NPC viability in FEFEFKFK SAPH. [A] LIVE/DEAD® assay for cell viability of 2×10^5 bNPCs ml^{-1} in 25 mg ml^{-1}, 30 mg ml^{-1} and 35 mg ml^{-1} FEFEFKFK SAPHs and 30 mg ml^{-1} alginate gels on days 1 and 7. Viable cells were stained green and dead cells were stained red. Scale bar represents 100 μm. [B] Percentage viable bNPCs present in LIVE/DEAD assay fluorescence micrographs for 25 mg ml^{-1}, 30 mg ml^{-1} and 35 mg ml^{-1} FEFEFKFK SAPHs on days 1 and 7. ($^{*}P < 0.05$, $^{***}P < 0.001$) Values expressed as mean ± SD where n = 3. [C] Percentage viable bNPCs present in LIVE/DEAD assay fluorescence micrographs for 30 mg ml^{-1} FEFEFKFK SAPHs, the concentration chosen for cell culture experiments, over 14 day culture. ($^{*}P < 0.05$). Values expressed as mean ± SD where n = 3. [D] Total viable cell population for 2×10^5 bNPCs ml^{-1} in 30 mg ml^{-1} FEFEFKFK SAPH and 30 mg ml^{-1} alginate gel. Values expressed as mean ± SD where n = 4. (For interpretation of the references to colour in this figure legend, the reader is referred to the web version of this article.)

3.4. Determining cell gene expression using conventional and NP-specific markers

Following culture of bNPCs in FEFEFKFK SAPH, expression of the conventional NP markers *COL2A1* and *SOX9*, and novel NP-specific markers *KRT8*, *KRT18* and *FOXF1* significantly increased from days 1–14 ($^{***}P < 0.001$) (Fig. 4A). *COL1A2* gene expression remained consistently low; around 45 times lower than *COL2A1* and 130 times lower than *ACAN* on day 14. The ratio of *ACAN* to *COL2A1* expression was 3:1 on day 14. Expression of *CA12* was not significantly influenced by culture time in FEFEFKFK SAPH.

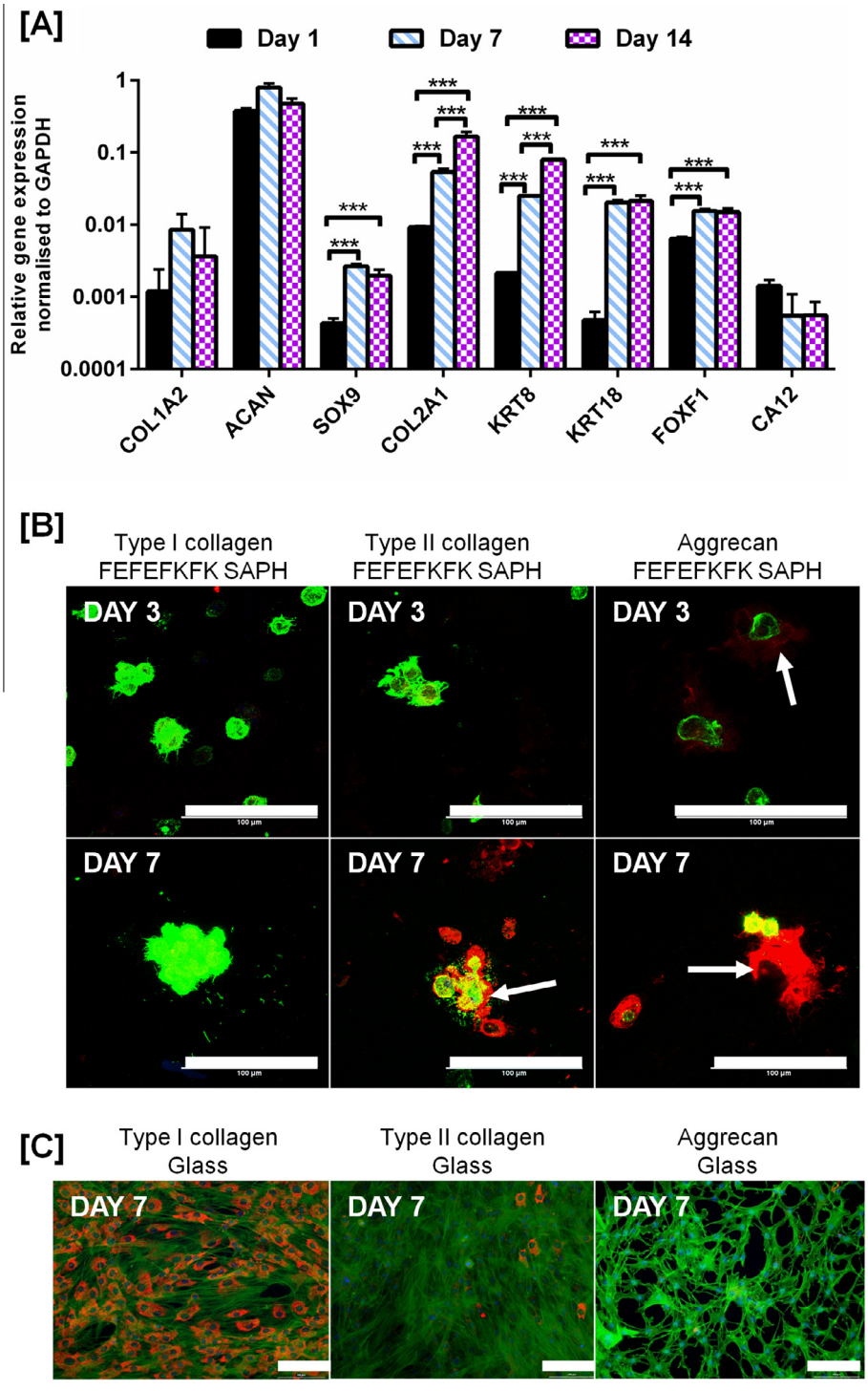

Fig. 4. [A] Gene expression for conventional NP markers (*COL1A2*, *ACAN*, *SOX9*, *COL2A1*) and NP-specific markers (*KRT8*, *KRT18*, *FOXF1*, *CA12*) for 1.5×10^6 bNPCs ml^{-1} in 30 mg ml^{-1} FEFEFKFK SAPHs on days 1, 7 and 14. Gene expression was normalised to *GAPDH*. ($^{***}P < 0.001$). Values expressed as mean ± SE where n = 4. [B] ICC for 2×10^5 bNPCs ml^{-1} in 30 mg ml^{-1} FEFEFKFK SAPH. White arrows highlight extracellular matrix deposition. Type I collagen, type II collagen and aggrecan were stained red, F-actin was stained green and cell nuclei were stained blue. Scale bar represents 100 µm. [C] ICC for 2×10^5 bNPCs ml^{-1} on glass monolayer culture on day 7. Type I collagen, type II collagen and aggrecan was stained red, F-actin was stained green and cell nuclei were stained blue. Scale bar represents 100 µm. (For interpretation of the references to colour in this figure legend, the reader is referred to the web version of this article.)

3.5. Visualising the deposition of NP-associated ECM components

Minimal type I collagen staining was observed on day 3 and day 7 when bNPCs were cultured in FEFEFKFK SAPHs (Fig. 4B). There was intense pericellular staining for type II collagen and aggrecan on day 7 for bNPCs cultured in FEFEFKFK SAPHs. Objectively, there was a time-dependent increase in amounts of type II collagen and aggrecan staining.

In contrast, bNPCs cultured on glass adopted a fibroblastic morphology (Fig. 4C). There was intense staining for type I collagen, minimal staining for type II collagen and no positive aggrecan staining.

3.6. Quantification of s-GAG

There was a significant increase in total s-GAG accumulation from days 1 (0.71 ± 0.06 μg) to 14 (1.72 ± 0.8 μg) ($^{**}P < 0.01$) (Fig. 5A). When total s-GAG accumulation per day was normalised with viable cell number in the sample, there was a significant increase in s-GAG production per cell from day 1 ($8.4 \times 10^{-3} \pm 1.9 \times 10^{-4}$ ng) to 14 (0.033 ± 0.017 ng) ($^{*}P < 0.05$) (Fig. 5B). No s-GAG was detected in pooled media which suggested that the majority of s-GAG was retained by the FEFEFKFK SAPH.

3.7. Compositional analysis of CS/DS

Metabolic radiolabel incorporation followed by targeted enzymatic digestion was used to focus on the specific contribution of CS and DS to the total GAG deposited by bNPCs during culture. Digestion generates an unsaturated uronic acid therefore the iduronic/glucuronic acid ratio could not be calculated using this method. CS/DS chain composition was not significantly different between samples (Fig. 5C). The overall GAG composition was approximately 45.9 ± 8.8% ΔUA-GalNAc(4S), (A unit), 42.7 ± 9.6% ΔUA-GalNAc(6S), (C unit), 9.3 ± 2.1% ΔUA-GalNAc (O unit) and 2.15 ± 0.42% ΔUA-GalNAc(4, 6S)/ΔUA-(2S)GalNAc(6S) (D and E units). There was no significant difference in ratio of A unit to C unit with the ratio approximately 1 to 1.

4. Discussion

In this study, the potential of FEFEFKFK SAPH as a cell delivery system and scaffold for NP tissue engineering was investigated. There are a number of important parameters to consider for potential NP biomaterial scaffolds including comparable mechanical properties to the native tissue, the ability of the system to be delivered via minimally invasive procedure, biocompatibility,

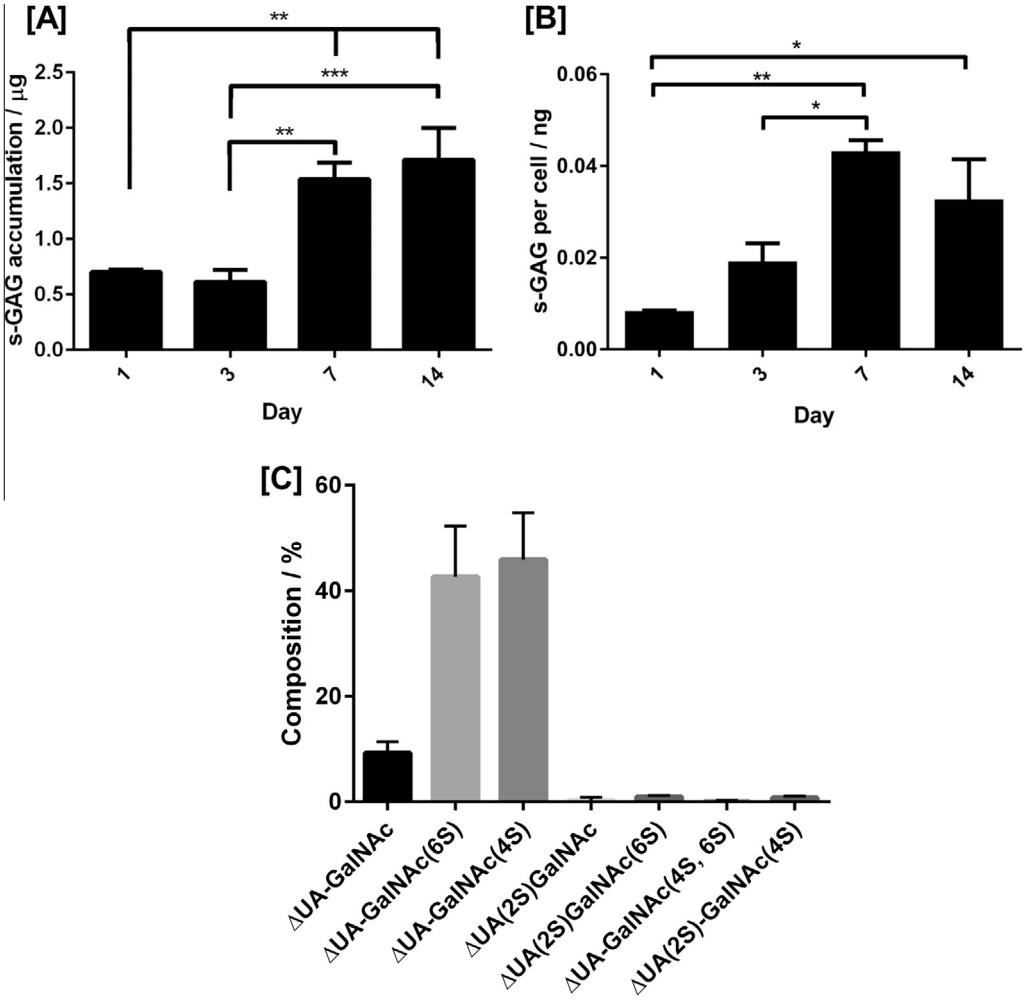

Fig. 5. Quantification of ECM components. [A] Total s-GAG accumulation in samples for 1.5×10^6 bNPC ml^{-1} in 30 mg ml^{-1} FEFEFKFK SAPHs. s-GAG accumulation was calculated from a standard graph plotting absorbance against standard s-GAG concentrations. ($^{**}P < 0.01$, $^{***}P < 0.001$). Values expressed as mean ± SD where n = 4. [B] Normalised s-GAG production per cell at a seeding density of 1.5×10^6 bNPC ml^{-1} in 30 mg ml^{-1} FEFEFKFK SAPHs. The total accumulated s-GAG in samples was divided by viable cell number on corresponding time point to estimate s-GAG production per cell. ($^{*}P < 0.05$, $^{**}P < 0.01$). Values expressed as mean ± SD where n = 4. [C] CS/DS disaccharide composition of 1.5×10^6 bNPCs ml^{-1} in 30 mg ml^{-1} FEFEFKFK SAPHs on day 7. CS/DS was extracted from 3 individual FEFEFKFK SAPHs containing bNPCs. Values expressed as mean ± SD. Sample A, n = 4 HPLC runs; Sample B n = 2 HPLC runs; Sample C n = 2 HPLC runs.

restoration and preservation of the NP phenotype and stimulation of appropriate ECM production.

Oscillatory rheology determined that FEFEFKFK SAPH concentration was proportional to system stiffness (Fig. 1A) as an increase in fibre density caused more fibre associations and entanglements [25,36]. All concentrations of acellular and cell-laden FEFEFKFK SAPHs experienced reductions in G′ and G″ with increasing timepoint (Fig. 1B) likely caused by degradation of the system due to the very high water content and its relative weakness. Cells are also likely to have produced various factors and enzymes that reduced the stability of the scaffold [40]. Reducing FEFEFKFK SAPH degradation i.e. by changing the peptide chain charge would be a worthwhile investigation to improve the stability of the system over long term culture. The NP has a crucial mechanical role [9] therefore it was important to try and match the biomechanical properties of FEFEFKFK SAPH to that of the native tissue. The native human NP modulus, ranging from 5.39 kPa [7] to 20 kPa [8], could be replicated by varying the FEFEFKFK SAPH concentration (Fig. 1A). Systems with insufficient mechanical properties are likely to fail after implantation whilst the transfer of loads to the AF might be ineffective. Systems that are too rigid could prevent pericellular remodelling which is crucial for the health of cells [40] and could accelerate DDD. The δ value of the FEFEFKFK SAPH was a better match to the native NP than other NP tissue engineering studies, for example Chen et al. HA-gelatin hydrogel had δ values of between 0 to 3° meaning that was dominant elastic with little viscous properties [41]. IVD surgery can accelerate DDD [42,43] therefore a cell-based therapy should be deliverable via minimally invasive implantation [7,42] to minimise damage to the AF and to fill irregularly shaped defects [44]. After shearing, the FEFEFKFK SAPH behaved more like a liquid (G″ > G′) however became more solid-like (G′ > G″) [38] within 6 s. This suggested that the system could be injectable as it flowed when submitted to shear stress i.e. through a small bore needle, then recovered its original stiffness when the shear stress was removed. A number of other studies on FEFEFKFK SAPH [36] and similar SAPHs [46] support the hypothesis that shear-thinning and self-healing systems are injectable. The FEFEFKFK SAPH shear thinning mechanism has not been extensively investigated, but as demonstrated by β-hairpin SAPHs, it could involve the nanofibre network fracturing to allow flow of material [45] with the self-healing mechanism caused by domains immediately percolating after removal of strain [45,46]. Shear thinning and self-healing systems do not rely on external stimuli to trigger the sol-gel transition [34] therefore should reduce leakage from the site of implantation [45]. The recovery cycles did not have a significant adverse effect on cell numbers (Fig. 2B) as NPCs are exposed to high hydrostatic and osmotic pressures in the native tissue [8,47]. This is in agreement with previous studies where the injection process had little impact on cell viability or distribution [45].

Biocompatibility of FEFEFKFK SAPH was assessed and it was determined that 30 mg ml^{-1} concentration supported the highest NPC viability (Fig. 3A & B) possibly due to system stiffness being most comparable to the native NP, placing cells in the most biomechanically appropriate microenvironment (Fig. 1A). High cell viability over *in vitro* culture, as demonstrated in Fig. 3C, is a requirement for NP tissue engineering strategies. Similar viability results demonstrating no significant differences between time points were recorded for the culture of rabbit NPCs in LN-NS SAPH (~89% on day 7) [30] and human NPCs in RAD-RAK SAPH (~86% on day 7) [31]. The characteristic NPC rounded morphology [48] was maintained in FEFEFKFK SAPHs (Fig. 3A), comparable to NPCs in the native tissue [49] and was a distinct morphologic alteration from the fibroblast-like morphology of monolayer culture. Viability and morphology were similar to other NP tissue engineering studies using a variety of biomaterial scaffolds [50–52] and for bNPCs cultured in alginate controls (Fig. 3A & D). Alginate controls displayed a significant time-dependent loss of stability therefore day 14 data was not available.

NPCs will only significantly proliferate when under stress [53], when cultured in monolayer [54] or during DDD [55] which leads to decreased type II collagen and aggrecan production and increased type I collagen production [56]. Crucially ECM deposition is also decreased when cells are in the proliferative state [51,57]. The main goal of the FEFEFKFK SAPH was to stimulate appropriate ECM production for tissue regeneration [30] and to regulate cell behaviour [58]. Therefore the stable viable cell population (Fig. 3D) was not of particular concern as NPCs were behaving, in terms of proliferation, as they would in the native tissue. Interestingly, most published papers investigating the culture of NPCs in SAPHs did not carry out cell number quantification assays [29–31]. There was an initial drop in viable cell numbers during seeding and plating the FEFEFKFK SAPH due to the basic nature of the culture environment likely inducing pH shock for some bNPCs. However after the pH levels were returned to more physiologically relevant levels following media washes (Section 2.4), no significant amounts of cell death occurred which suggested that the FEFEFKFK SAPH at pH 7.4 was a suitable culture environment.

NPCs lose their phenotypic characteristics during monolayer culture as *COL2A1*and *ACAN* expression is downregulated [54] whilst *COL1A2* expression increases [59]. Therefore it is crucial that NP tissue engineering scaffolds are able to re-differentiate NPCs. The significant gene expression increases with culture period of conventional NP markers *SOX9* and *COL2A1* and the NP-specific markers *KRT8*, *KRT18* and *FOXF1* strongly suggested that FEFEFKFK SAPH could restore and preserve the NP phenotype throughout *in vitro* culture (Fig. 4A). Only one previous NP tissue engineering study has used as extensive a panel of NP markers; Kim et al. detected time-dependent significant increases in *KRT8* and *KRT18* gene expression [48] after the culture of bNPCs in HA hydrogels. The *ACAN* to *COL2A1* expression ratio from freshly harvested NPCs cultured in monolayer has been reported at 1:1 [60]. However in the native NP, the aggrecan to type II collagen ratio at the protein level has been reported as 27:1 [61]. Deposition of aggrecan and type II collagen are closely related to the cellular corresponding gene expression levels [30,62]. On day 14, the *ACAN* to *COL2A1* ratio for this study was higher in comparison to the culture of NPCs in HA gels after 28 days [48] or LN-NS SAPH after 14 days [30] where both studies reported a ratio of around 1:1. This suggested that a more gelatinous matrix was being produced by NPCs cultured in FEFEFKFK SAPHs.

ICC determined that NPCs cultured in FEFEFKFK SAPH deposited the vital NP ECM components of type II collagen and aggrecan extracellularly (Fig. 4B). Type I collagen, which is produced by NPCs from degenerated IVDs [59], was not significantly produced (Fig. 4B). In contrast, monolayer culture stimulated NPCs to produce type I collagen with no significant type II collagen or aggrecan deposition (Fig. 4C). It was evident from ICC micrographs that to ensure phenotypic stability of NPCs and production of NP associated ECM components, three-dimensional culture in an appropriate scaffold was essential [63].

Quantitative measurement of s-GAGs from PGs, with aggrecan the most prevalent in the NP, demonstrated a significant time-dependent increase in s-GAG accumulation and normalised NPC s-GAG production (Fig. 5A & B). Results supported our hypothesis that stable viable NPC population was not of major concern as appropriate ECM deposition could take place in absence of cellular proliferation. Significant increases in normalised s-GAG to DNA ratios were reported for NPCs cultured in HA hydrogels [48], alginate [64] and KLD-12 SAPHs (from days 1–7) [29] with these studies reporting significantly higher s-GAG accumulation that

the presented study. This was likely explained by the higher initial cell-seeding densities used by the comparable studies ranging from 4×10^6 cells ml^{-1} [64] to 60×10^6 cells ml^{-1} [48]. Increasing cell seeding density has been demonstrated to directly correlate with an increase in s-GAG accumulation [65]. No s-GAG was detected in the pooled media which suggested that the FEFEFKFK SAPH was effective in retaining synthesised PGs. Bringing together the *ACAN* gene expression results with the increasing levels of total s-GAG, it was likely that there was an increase in aggrecan deposition by the bNPCs during culture in the SAPH and this may also have been the case for other ECM components. A number of NP tissue engineering studies demonstrated time-dependent increases in *ACAN* and *COL2A1* expression accompanied by increasing corresponding protein deposition [48,59]. Therefore it was likely that the higher *ACAN* to *COL2A1* expression ratio (Fig. 4A) meant that more aggrecan than type II collagen was deposited at the protein level, however a type II collagen quantification assay would be required to confirm this hypothesis. ICC (Fig. 4B) and s-GAG quantification assays (Fig. 5A & B) demonstrated that NP-associated ECM components were deposited by bNPCs over the culture period however due to the low cell-seeding density and length of study it was unlikely that the matrix contributed to overall SAPH integrity as demonstrated by the decrease in mechanical properties over culture period (Fig. 1B).

Aggrecan consists of keratan sulphate chains, and CS/DS chains enriched in UA-GalNAc(4S) A unit and UA-GalNAc(6S) C unit type disaccharides [66]. UA-GalNAc(6S) was found to be the most prevalent s-GAG disaccharide in bovine NPs [67] however our study demonstrated that there was no significant difference between A and C unit contribution after culture of bNPCs in FEFEFKFK SAPHs (Fig. 5C). Quantification of GAG production by NPCs in potential tissue engineering scaffolds has not been extensively investigated, however Horner et al. determined that there was intense ICC staining extracellularly for both A unit and C unit by bNPCs cultured in alginate gels [68] and Maldonado et al. determined that the GAG composition for canine NPCs in alginate beads was 31% A unit, 61% C unit and 8% E unit [69]. Both UA-GalNAc(4S) and UA-GalNAc(6S) are present in human NP ECM in varying amounts dependent on age. At 1–4 years old, the ratio between UA-GalNAc(4S) and UA-GalNAc(6S) is around 2:1 with UA-GalNAc(4S) becoming dominant at older ages [70]. CS/DS levels and sulphation patterning is tissue-specific [71], linked to PG function and strongly influenced by the microenvironment therefore monitoring of CS/DS profiles of encapsulated cells and comparison with those of the native NP is a useful additional measure of likely therapeutic use.

Transplantation of NPCs into degenerated NPs has produced promising results with regards to the treatment of DDD and LBP [17,21]. Our research first focused on optimisation and characterisation of FEFEFKFK SAPH then NPC culture was investigated, as the application of FEFEFKFK SAPH for NP tissue engineering was previously untested. We hypothesised that the nanofibrous architecture [25] and optimised mechanical properties of the FEFEFKFK SAPH mimicked the native NP ECM. The culture environment directed NPCs to re-differentiate and preserve their phenotype after encapsulation as evidenced by upregulation of recently identified NP-specific genes and stimulated production of crucial NP-associated ECM components which were detected by a wide range of analytical techniques. Data suggested that FEFEFKFK SAPH could be used to deliver NPCs into degenerate NPs where transplanted cells would restore native ECM for the treatment of DDD and LBP. This study acted as crucial background work for progression of research towards the culture of human mesenchymal stem cells (MSCs), currently regarded to be one of the most promising NP tissue engineering cell sources [12], in FEFEFKFK SAPH. It was essential to study the response of NPCs in the system as ultimately differentiation of MSCs to a NP-like phenotype is required. Further characterisation of the system will be needed to determine the effect of scaffold properties (such as pH and stiffness) on MSCs and to promote their differentiation towards the NP-like phenotype.

5. Conclusion

Presented results supported the hypothesis that FEFEFKFK SAPH could be used as a NPC carrier and scaffold for NP tissue engineering. Characterisation and optimisation of the FEFEFKFK SAPH demonstrated that the native NP strength could be closely replicated and the system displayed shear-thinning and self-healing properties which indicated that it was likely deliverable via a minimally invasive procedure. From a cell biology standpoint, upregulation of NP-specific genes confirmed that the system restored the NP phenotype following monolayer culture de-differentiation and the discogenic phenotype was preserved throughout *in vitro* culture. High NPC viability was supported for the duration of experiments and NPCs were stimulated into depositing NP-associated ECM components. We hypothesised that the comparable mechanical properties of the FEFEFKFK SAPH to the native NP as well as the nanofibrous architecture of the system mimicked the native ECM and provided a suitable microenvironment for NPCs and thus suggests that the system holds potential as a cell-based therapy for NP tissue engineering and is fully deserving of further investigation.

Acknowledgements

The authors would like to thank EPSRC (UK) for financial support of the project through a School of Materials DTA award.

References

[1] W.F. Stewart, J.A. Ricci, E. Chee, D. Morganstein, R. Lipton, Lost productive time and cost due to common pain conditions in the US workforce, JAM 290 (18) (2003) 2443–2454.
[2] N. Maniadakis, A. Gray, The economic burden of back pain in the UK, Pain 84 (1) (2000) 95–103.
[3] F.M. Williams, A.T. Bansal, J.B. Meurs, J.T. Bell, I. Meulenbelt, P. Suri, F. Rivadeneira, P.N. Sambrook, A. Hofman, S. Bierma-Zeinstra, C. Menni, M. Kloppenburg, P.E. Slagboom, D.J. Hunter, A.J. MacGregor, A.G. Uitterlinden, T.D. Spector, Novel genetic variants associated with lumbar disc degeneration in northern Europeans: a meta-analysis of 4600 subjects, Ann. Rheum. Dis. 72 (2013) 1141–1148.
[4] J.P.G. Urban, S. Roberts, Degeneration of the intervertebral disc, Arthritis Res. Ther. 5 (3) (2003) 120–131.
[5] K.M. Cheung, J. Karppinen, D. Chan, D.W. Ho, Y.-Q. Song, P. Sham, K.S. Cheah, J. C. Leong, K.D. Luk, Prevalence and pattern of lumbar magnetic resonance imaging changes in a population study of one thousand forty-three individuals, Spine 34 (9) (2009) 934–940.
[6] M.D. Humzah, R.W. Soames, Human intervertebral disc: structure and function, Anat. Rec. 220 (4) (1988) 337–356.
[7] J.M. Cloyd, N.R. Malhotra, L. Weng, W. Chen, R.L. Mauck, D.M. Elliott, Material properties in unconfined compression of human nucleus pulposus, injectable hyaluronic acid-based hydrogels and tissue engineering scaffolds, Eur. Spine J. 16 (11) (2007) 1892–1898.
[8] J.C. Iatridis, L.A. Setton, M. Weidenbaum, V.C. Mow, The viscoelastic behaviour of the non-degenerate human lumbar nucleus pulposus in shear, J. Biomech. 30 (10) (1997) 1005–1013.
[9] M.A. Adams, Biomechanics of back pain, Acupunct. Med. 22 (4) (2004) 178–188.
[10] C.L. Le Maitre, A.J. Freemont, J.A. Hoyland, The role of interleukin-1 in the pathogenesis of human intervertebral disc degeneration, Arthritis Res. Ther. 7 (4) (2005) 732–744.
[11] D. Sakai, S. Grad, Advancing the cellular and molecular therapy for intervertebral disc disease, Adv. Drug Deliv. Rev. 84 (2014) 159–171.
[12] H.T. Gilbert, J.A. Hoyland, S.M. Richardson, Stem cell regeneration of degenerated intervertebral discs: current status, Curr. Pain Headache Rep. 17 (12) (2013) 1–9.
[13] J.K. Freburger, G.M. Holmes, R.P. Agans, A.M. Jackman, J.D. Darter, A.S. Wallace, L.D. Castel, W.D. Kalsbeek, T.S. Carey, The rising prevalence of chronic low back pain, Arch. Intern. Med. 169 (3) (2009) 251–259.

[14] C.J. Hunter, J.R. Matyas, N.A. Duncan, The notochordal cell in the nucleus pulposus: a review in the context of tissue engineering, Tissue Eng. 9 (4) (2003) 667–678.
[15] J. Mochida, D. Sakai, Y. Nakumura, T. Watanabe, Y. Yamamoto, S. Kato, Intervertebral disc repair with activated nucleus pulposus cell transplantation: a three year, prospective clinical study of its safety, Eur. Cells Mater. 29 (2015) 202–212.
[16] K.D. Hudson, M. Alimi, P. Grunert, R. Hartl, L.J. Bonassar, Recent advances in biological therapies for disc degeneration: tissue engineering of the annulus fibrosus, nucleus pulposus and whole intervertebral disc, Biotechnology 24 (5) (2013) 872–879.
[17] D. Oehme, T. Goldschlager, P. Ghosh, J.V. Rosenfeld, G. Jenkin, Cell based therapies used to treat lumbar degenerative disc disease; a systematic review of animal studies and human clinical trials, Stem Cell Int. (2015) 1–15.
[18] T. Ganey, L. Libera, V. Moos, O. Alasevic, K.G. Fritsch, H.J. Meisel, W.C. Hutton, Disc chondrocyte transplantation in a canine model: a treatment for degenerated or damaged intervertebral disc, Spine 28 (23) (2003) 2609–2620.
[19] C. Hohaus, T.M. Ganey, Y. Minkus, H.J. Meisel, Cell transplantation in lumbar spine disc degeneration disease, Eur. Spine J. 17 (4) (2008) 492–503.
[20] H.J. Meisel, V. Siodla, T. Ganey, Y. Minkus, W.C. Hutton, O.J. Alasevic, Clinical experience in cell-based therapeutics: disc chondrocyte transplantation: a treatment for degenerated or damaged intervertebral disc, Biomol. Eng. 24 (1) (2007) 5–21.
[21] H.J. Meisel, T. Ganey, W.C. Hutton, J. Libera, Y. Minkus, O.J. Alasevic, Clinical experience in cell-based therapeutics: intervention and outcome, Eur. Spine J. 15 (3) (2006) 397–405.
[22] A.F. Miller, A. Saiani, Engineering peptide based biomaterials: structure, properties and application, Chem. Today 28 (1) (2010) 34–38.
[23] M. Nune, P. Kumaraswamy, U. Krishnan, S. Sethuraman, Self-assembling peptide nanofibrous scaffolds for tissue engineering: novel approaches and strategies for effective functional regeneration, Curr. Protein Pept. Sci. 14 (1) (2013) 70–84.
[24] S. Boothroyd, A. Saiani, A.F. Miller, Formation of mixed ionic complementary peptide fibrils, Macromol. Symp. 273 (2008) 139–145.
[25] A. Saiani, A. Mohammed, N. Frielinghaus, R. Collins, N. Hodson, C.M. Kielty, M.J. Sherratt, A.F. Miller, Self-assembly and gelation properties of α-helix versus β-sheet forming peptides, Soft Matter 5 (1) (2009) 193–202.
[26] J. Kisiday, M. Jin, B. Kurz, H. Hung, C. Semino, S. Zhang, A.J. Grodzinsky, Self-assembling peptide hydrogel fosters chondrocyte extracellular matrix production and cell division: implications for cartilage tissue repair, PNAS 99 (15) (2002) 9996–10001.
[27] L.A.C. Diaz, A. Saiani, J.E. Gough, A.F. Miller, Human osteoblasts within soft peptide hydrogels promote mineralisation in vitro, J. Tissue Eng. 5 (2014) 1–12.
[28] S. Zhang, H. Yokoi, F. Gelain, A. Horii, Designer self-assembling peptide nanofibre scaffolds, in; Nanotechnology for Biology and Medicine: At the Building Block Level, 2012, pp. 123–147.
[29] J. Sun, Q. Zheng, Y. Wu, Y. Liu, X. Guo, W. Wu, Culture of nucleus pulposus cells from intervertebral disc on self-assembling KLD 12 peptide hydrogel scaffold, Mater. Sci. Eng. 30 (7) (2010) 975–980.
[30] B. Wang, Y. Wu, Z. Shao, S. Yang, B. Che, C. Sun, Z. Ma, Y. Zhang, Functionalized self-assembling peptide nanofiber hydrogel as a scaffold for rabbit nucleus pulposus cells, J. Biomed. Mater. Res. 100 (3) (2012) 643–653.
[31] H. Tao, Y. Zhang, C.F. Wang, C. Zhang, X.M. Wang, D.L. Wang, X.D. Bai, T.Y. Wen, H.K. Xin, J.H. Wu, Y. Liu, Q. He, D. Ruan, Biological evaluation of human degenerated nucleus pulposus cells in functionalised self-assembling peptide nanofibre hydrogel scaffold, Tissue Eng. 20 (2014) 1621–1722.
[32] H. Tao, Y. Wu, H. Li, C. Wang, Y. Zhang, C. Li, T. Wen, X. Wang, Q. He, D. Wang, D. Ruan, BMP7-based functionalised self-assembling peptides for nucleus pulposus tissue engineering, Appl. Mater. Interfaces 7 (31) (2015) 17076–17087.
[33] B.M. Minogue, S.M. Richardson, L.A. Zeef, A.J. Freemont, J.A. Hoyland, Transcriptional profiling of bovine intervertebral disc cells: implications for identification of normal and degenerate human intervertebral disc cell phenotypes, Arthritis Res. 12 (2010) 1–20.
[34] C. Tang, A.F. Miller, A. Saiani, Peptide hydrogels as mucoadhesive for local drug delivery, Int. J. Pharm. 465 (1) (2014) 427–435.
[35] L. Szkolar, J.B. Guilbaud, A.F. Miller, J.E. Gough, A. Saiani, Enzymatically triggered peptide hydrogels for 3D cell encapsulation and culture, J. Pept. Sci. 20 (7) (2014) 578–584.
[36] A. Mujeeb, A.F. Miller, A. Saiani, J.E. Gough, Self-assembled octapeptide scaffolds for in vitro chondrocyte culture, Acta Biomater. 9 (1) (2012) 4609–4619.
[37] J.I. Sive, P. Baird, M. Jeziorsk, A. Watkins, J.A. Hoyland, A.J. Freemont, Expression of chondrocyte markers by cells of normal and degenerate intervertebral discs, J. Clin. Pathol. Mol. Pathol. 55 (2002) 91–97.
[38] C. Yan, D.J. Pochan, Rheological properties of peptide-based hydrogels for biomedical and other applications, Chem. Soc. Rev. 39 (2010) 3528–3540.
[39] C.E. Johnson, B.E. Crawford, M. Stavridis, Dam.G. Ten, A.L. Wat, G. Rushton, C.M. Ward, V. Wilson, T.H. van Kuppevelt, J.D. Esko, A. Smith, J.T. Gallagher, C.L. Merry, Essential alterations of heparan sulfate during the differentiation of embryonic stem cells to Sox1-enhanced green fluorescent protein-expressing neural progenitor cells, Stem Cells 25 (8) (2007) 1913–1923.
[40] A.I. Chou, S.B. Nicoll, Characterisation of photocrosslinked alginate hydrogels for nucleus pulposus cell encapsulation, Wiley InterScience 91(1) (2009) 187–195.
[41] Y.C. Chen, W.Y. Su, S.H. Yang, A. Gefen, F.H. Lin, In situ forming hydrogels composed oxidised high molecular weight hyaluronic acid and gelatine for nucleus pulposus regeneration, Acta Biomater. 9 (2) (2012) 5181–5193.
[42] R. Kandel, S. Roberts, J.P.G. Urban, Tissue engineering and the intervertebral disc: the challenges, Eur. Spine J. 17 (4) (2008) 480–491.
[43] D.R. Pereira, J. Silva-Correia, J.M. Oliveira, R.L. Reis, Hydrogels in acellular and cellular strategies for intervertebral disc regeneration, J. Tissue Eng. Regen. Med. 7 (2) (2011) 85–98.
[44] E.C. Collin, S. Grad, D.I. Zeugolis, C.S. Vinatier, J.R. Clouet, J.J. Guicheux, P. Weiss, M. Alini, A.S. Pandit, An injectable vehicle for nucleus pulposus cell-based therapy, Biomaterials 32 (11) (2011) 2862–2870.
[45] C. Yan, A. Altunbas, T. Yucel, R.P. Nagarkar, J.P. Schneider, D.J. Pochan, Injectable solid hydrogel: mechanism of shear-thinning and immediate recovery of injectable β-hairpin peptide hydrogels, Soft Matter 6 (20) (2010) 5143–5156.
[46] F. Gelain, D. Silva, A. Caprini, F. Taraballi, A. Natalello, O. Villa, K.T. Nam, R.N. Zuckerman, S.M. Doglia, A. Vescovi, BMHP1-derived self-assembling peptides: hierarchically assembled structures with self-healing propensity and potential for tissue engineering applications, ACS Nano 5 (3) (2011) 1845–1859.
[47] M.A. Adams, P.J. Roughley, What is intervertebral disc degeneration and what causes it?, Spine 31 (18) (2006) 2151–2161
[48] D.H. Kim, J.T. Martin, D.M. Elliott, L.J. Smith, R.L. Mauck, Phenotypic stability, matrix elaboration and functional maturation of nucleus pulposus cells encapsulated in photocrosslinkable hyaluronic acid hydrogels, Acta Biomater. 12 (2015) 21–29.
[49] S. Roberts, H. Evans, J. Trivedi, J. Menage, Histology and pathology of the human intervertebral disc, J. Bone Joint Surg. 88 (2) (2006) 10–14.
[50] C. Witsey, P. Kubinski, T. Christiani, K. Toomer, J. Sheehan, A. Branda, J. Kadlowee, C. Iftode, J. Vernego, Characterisation of injectable hydrogels based on poly(N-isopropylacrylamide)-g-chondroitin sulphate with adhesive properties for nucleus pulposus tissue engineering, J. Mater. Sci. 24 (4) (2013) 837–847.
[51] B.L. Foss, T.W. Maxwell, Y. Deng, Chondroprotective supplementation promotes the mechanical properties of injectable scaffold for human nucleus pulposus tissue engineering, J. Biomech. Mater. 24 (2014) 56–67.
[52] M. Peroglio, S. Grad, D. Mortisen, C.M. Sprecher, S. Junger, M. Alini, D. Eglin, Injectable thermoreversible hyaluronan-based hydrogels for nucleus pulposus cell encapsulation, Eur. Spine J. 21 (6) (2011) 839–849.
[53] C.A. Sharp, S. Roberts, H. Evans, S.J. Brown, Disc cell clusters in pathological human intervertebral discs are associated with increased stress protein immunostaining, Eur. Spine J. 18 (11) (2009) 1587–1594.
[54] T. Kluba, T. Niemeyer, C. Gaissmaier, T. Grunder, Human annulus fibrosus and nucleus pulposus cells of the intervertebral disc, Spine 30 (24) (2005) 2743–2748.
[55] W.E. Johnson, S.M. Eisenstein, S. Roberts, Cell cluster formation in degenerate lumbar intervertebral discs is associated with increased disc cell proliferation', Connect. Tissue Res. 42 (3) (2001) 197–207.
[56] C.L. LeMaitre, A. Pockert, D.J. Buttle, A.J. Freemont, J.A. Hoyland, Matrix synthesis and degradation in human intervertebral disc degeneration, Biochem. Soc. Trans. 35 (4) (2007) 652–655.
[57] K.I. Lee, S.H. Moon, H. Kim, U.H. Kwon, H.J. Kim, S.N. Park, H. Sun, H.S. Lee, H.J. Kim, H.J. Chun, I.K. Kwon, J.W. Jang, Tissue engineering of the intervertebral disc with cultured nucleus pulposus cells using atelocollagen scaffold and growth factors, Spine 37 (6) (2012) 452–458.
[58] M.W. Tibbitt, K.S. Anseth, Hydrogels as extracellular matrix mimics for 3D cell culture, Biotechnol. Bioeng. 103 (4) (2009) 655–663.
[59] A.I. Chou, A.T. Reza, S.B. Nicoll, Distinct intervertebral disc cell populations adopt similar phenotypes in three-dimensional culture, Tissue Eng. 14 (12) (2008) 2070–2089.
[60] J.Y. Park, S.U. Kuh, H.S. Park, K.S. Kim, Comparative expression of matrix associated genes and inflammatory cytokines-associated genes according to disc denegation: analysis of living human nucleus pulposus, J. Spinal Disord. Tech. 24 (6) (2011) 352–357.
[61] F. Mwale, P. Roughley, J. Antoniou, Distinction between the extracellular matrix of the nucleus pulposus and hyaline cartilage: a requisite for tissue engineering of intervertebral disc, Eur. Cells Mater. 8 (2004) 58–64.
[62] F. Mwale, C.N. Demers, A. Petit, P. Roughley, A.R. Poole, T. Steffen, M. Aebi, J. Antoniou, A synthetic peptide of link protein stimulates the biosynthesis of collagens II, IX and proteoglycan by cells of the intervertebral disc, J. Chem. Biochem. 88 (6) (2003) 1202–1213.
[63] G. Feng, Z. Zhang, X. Jin, J. Hu, M.J. Gupte, J.M. Holzwarth, P.X. Ma, Regenerating nucleus pulposus of the intervertebral disc using biodegradable nanofibrous polymer scaffold, Tissue Eng. 18 (21) (2012) 1–8.
[64] S.M. Naqvi, C.T. Buckley, Extracellular matrix production by nucleus pulposus and bone marrow stem cells in response to altered oxygen and glucose microenvironments, J. Anat. 227 (2015) 757–766.
[65] S. Kobayashi, A. Meir, J. Urban, Effect of cell density on the rate of glycosaminoglycan accumulation by disc and cartilage cells in vitro, J. Orthop. Res. 26 (4) (2008) 493–503.
[66] J. Melrose, P. Ghosh, T.K. Taylor, A comparative analysis of the differential spatial and temporal distributions of the large (aggrecan, versican) and small (decorin, biglycan, fibromodulin) proteoglycans of the intervertebral disc, J. Anat. 198 (1) (2001) 3–15.
[67] L. Rosenberg, M. Schubert, The protein polysaccharides of bovine nucleus pulposus, J. Biol. Chem. 242 (20) (1967) 4691–4701.

[68] H.A. Horner, S. Roberts, R.C. Bielby, J. Menage, H. Evans, J.P. Urban, Cells from different regions of the intervertebral disc: effect of culture system on matrix expression and cell phenotype, Spine 27 (10) (2002) 1018–1028.
[69] B.A. Maldonado, T.R. Oegema, Initial characterisation of the metabolism of intervertebral disc cells in microspheres, J. Orthop. Res. 10 (5) (1992) 677–690.
[70] F. Postacchini, Lumbar Disc Herniation, SpringerWein, NewYork, 1999.
[71] X.N. Stachtea, E. Tykesson, T.H. van Kuppevelt, R. Feinstein, A. Malmstron, R.M. Reijmers, M. Maccarana, Dermatan sulfate-free mice display embryological defects and are neonatal lethal despite normal lymphoid and non-lymphoid organogenesis, PLoS One 10 (10) (2015) 1–20.